

## Abridgment

# Constitutive Relations and Failure Model for Plain Concrete and Steel-Fiber-Reinforced Concrete

M. REZA SALAMI

A constitutive model based on the theory of plasticity is proposed and utilized to characterize the stress-deformation behavior of plain concrete and steel-fiber-reinforced concrete. It allows for factors such as stress hardenings, volume changes, stress paths, cohesive and tensile strengths, and variation of yield behavior with mean pressure. It is applied to characterize behavior of plain concrete and steel-fiber-reinforced concrete. The constants for the model are determined from a series of available laboratory tests conducted under different initial confinements and stress paths obtained by using multiaxial and cylindrical triaxial testing devices. The model is verified with respect to observed laboratory responses. Overall, the proposed model is found suitable to characterize the behavior of plain concrete and steel-fiber-reinforced concrete.

Characterization of the stress-deformation behavior of concrete has long been a subject of active research. Linear elastic, nonlinear (piecewise linear) elastic, elastic-plastic, and endochronic models have been proposed and used by various investigators, and the literature on the subject is extensive. An excellent review of various models together with their implementation in numerical (finite element) procedures is presented by the subcommittee on the subject chaired by Chen et al. (1) This paper presents a general model to characterize ultimate (and failure) and hardening (softening) response in the context of the theory of plasticity.

## PROPOSED MODEL

One of the functions used to define yield function in the context of incremental plasticity (2,3) is given by

$$J_{2D} + \alpha J_1^2 - \beta J_1 J_3^{1/3} - \gamma J_1 - k^2 = 0 \quad (1)$$

where  $J_{2D}$  is the second invariant of the deviatoric stress tensor, and  $\alpha$ ,  $\beta$ ,  $\gamma$ , and  $k$  are response functions. For the behavior of plain concrete and steel fiber concrete,  $\alpha$ ,  $\gamma$ , and  $k$  are associated with the ultimate surface, whereas  $\beta$  is adopted as the growth function (hardening). Figures 1a and 1b show plots of  $F$  in the  $(J_{2D})^{1/2}$   $J_1$  and triaxial planes for plain concrete, respectively.

To include the cohesion and the tensile strength in the ultimate criterion, a translation of the principal stress space along the hydrostatic axis is performed. A new yield function becomes

$$F = J_{2D}^* + \alpha J_1^{*2} - \beta J_1^* J_3^{*1/3} - \gamma J_1^* \quad (2)$$

For material at ultimate, Equation 2 becomes

$$J_{2D}^* + \alpha J_1^{*2} - \beta J_1^* J_3^{*1/3} - \gamma J_1^* = 0 \quad (3)$$

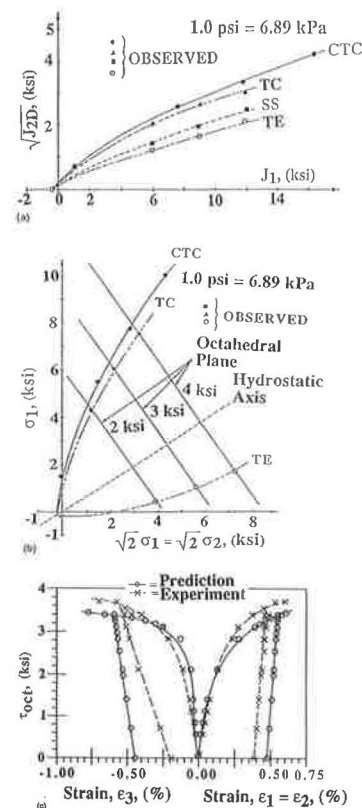


FIGURE 1 Observed ultimate surfaces: *a*, in  $(J_{2D})^{1/2} - J_1$  and *b*, in triaxial plane for plain concrete; *c*, comparison of stress-strain responses of triaxial extension test for plain concrete.

where

$$J_1^* = \sigma_{11}^* + \sigma_{22}^* + \sigma_{33}^* \quad (4a)$$

$$J_{2D}^* = \frac{1}{6} [(\sigma_{11}^* - \sigma_{22}^*)^2 + (\sigma_{22}^* - \sigma_{33}^*)^2 + (\sigma_{11}^* - \sigma_{33}^*)^2] + \sigma_{12}^{*2} + \sigma_{23}^{*2} + \sigma_{13}^{*2} \quad (4b)$$

$$J_3^* = \frac{1}{3} (\sigma_{11}^{*3} + \sigma_{22}^{*3} + \sigma_{33}^{*3}) \quad (4c)$$

The resulting normal ultimate stresses  $\sigma_{11}^*$ ,  $\sigma_{22}^*$ , and  $\sigma_{33}^*$  in equations 4a–c are then expressed as

$$\sigma_{11}^* = \sigma_{11} + R \quad (5a)$$

$$\sigma_{22}^* = \sigma_{22} + R \quad (5b)$$

$$\sigma_{33}^* = \sigma_{33} + R \quad (5c)$$

and

$$R = ap_a \quad (6)$$

where  $a$  = dimensionless number and  $p_a$  = atmospheric pressure. For cohesionless geological materials,  $R = 0$ , and the resulting ultimate function in Equation 2 reduces to Equation 1. If the uniaxial tensile strength ( $f_t$ ) is not determined experimentally, Salami (3) and Lade (4) give an approximate formula relating  $f_t$  to the unconfined compression strength ( $f_{cu}$ ) through the following power function as

$$f_t = mp_a(f_{cu}/p_a)^n \quad (7)$$

where

$m$  and  $n$  = dimensionless numbers,  
 $f_t$  = uniaxial tensile strength,  
 $f_{cu}$  = unconfined compression strength, and  
 $p_a$  = atmospheric pressure.

For concrete materials,  $m = 0.62$  and  $n = 0.68$ . Once  $f_t$  is known, the value of  $R$  can be estimated. With the estimated value of  $R$ , the resulting stresses in equations 5a–c are calculated and then substituted into the expressions of the stress invariants given by equations 4a–c. The parameters  $a$  and  $g$  for the ultimate surface are determined by substituting ultimate stresses for various stress paths in equations 4a–c and then substituting them in Equation 3. Hence, a set of simultaneous equations that can be solved is obtained.

### Growth Function, $\beta$

To define hardening and softening, the growth function is expressed as

$$\beta(\xi, r_D) = \beta_u \left[ 1 - \frac{\beta_a}{i + \xi^n [1 - \beta_b(r_D)^{n_2}]} \right] \quad (8)$$

where

$$\beta_u = 3\alpha,$$

$\beta_a$  and  $\eta_1$  = constants determined from hydrostatic compression tests,

$\beta_b$  and  $\eta_1$  = constants determined from shear or coupled (shear and volumetric) tests,

$i$  = elastic limit (for material showing plastic yielding from the beginning of loading  $i = 0$ ),

$\xi$  = trajectory of plastic strains

$$\xi = f(d\epsilon_{ij}^p d\epsilon_{ij}^p)^{1/2} \quad (9)$$

$r_D$  = the ratio of trajectory of deviatoric plastic strains

$\xi_D = f(dE_{ij}^p dE_{ij}^p)^{1/2}$  to  $\xi$ , and

$E_{ij}^p$  = deviatoric plastic strain tensor.

### Elastic Constants

The value of  $E$  is found as (average) slope of the unloading-reloading portion of the stress-strain curves; often the curves for the conventional triaxial compression (CTC) path are used for this purpose. The value of Poisson's ratio can be found from the measurements of the principal strains,  $\epsilon_1$ ,  $\epsilon_2$ , and  $\epsilon_3$ .

### APPLICATIONS

The behavior of both plain and steel-fiber-reinforced concrete is verified by using the proposed model. For plain concrete, the entire hardening and ultimate responses are modeled, whereas for steel-fiber-reinforced concrete only the ultimate (failure) behavior is considered. Comprehensive laboratory tests under various stress paths (Figure 2) using the multiaxial testing device (3) reported by Scavuzzo et al. (5) and Egging (6) are used.

The constants for the two materials were obtained by using the foregoing procedures. Their values are presented in Tables 1 and 2.

### VERIFICATION

The proposed model was verified by predicting laboratory test results under different stress paths. The incremental constitutive equations were integrated along a given stress path, starting from a given initial (hydrostatic) condition:

$$\{d\sigma\} = [C^{ep}]\{d\epsilon\} = ([C^e] - [C^p])\{d\epsilon\} \quad (10)$$

where  $\{d\sigma\}$  and  $\{d\epsilon\}$  are vectors of incremental stresses and strain, respectively, and  $[C^{ep}]$  is an elastic-plastic constitutive matrix with  $[C^e]$  as its elastic part and  $[C^p]$  as its plastic part. The latter was derived by using the theory of plasticity with  $F$  in Equation 2 as the yield function with the normality rule

$$d\epsilon_{ij} = \lambda(\partial F / \partial \sigma_{ij}) \quad (11)$$

and the consistency condition  $dF = 0$ ; here  $\lambda$  is a scalar proportionality parameter. Note that the matrix  $[C^{ep}]$  is ex-

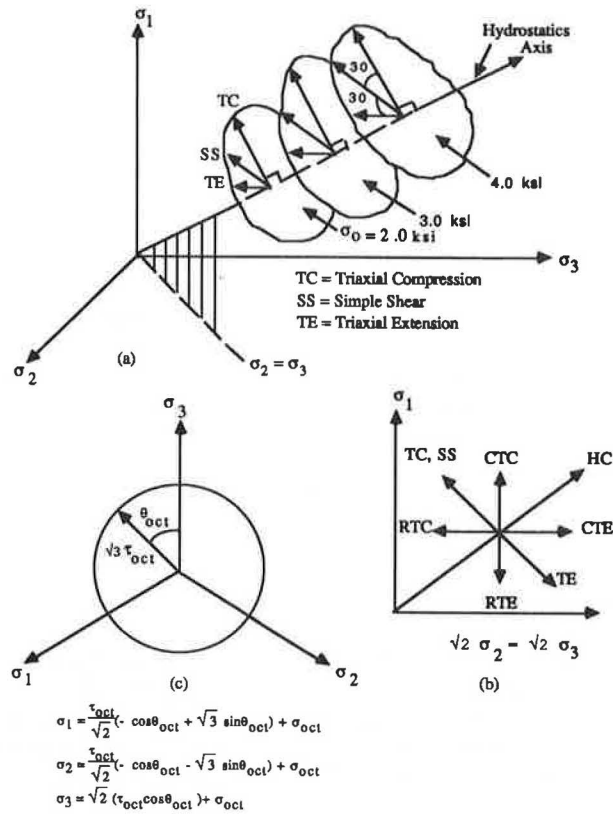


FIGURE 2 Commonly used stress paths in *a*, three-dimensional stress space and octahedral plane; *b*, triaxial plane; *c*, circular stress path with principal stress relations given (1.0 psi = 6.89 kPa) (compression stresses positive).

TABLE 1 MATERIAL CONSTANTS FOR PLAIN CONCRETE FROM DIFFERENT STRESS PATH TESTS

		English Units	SI Units
Elastic Constants	K	2000 ksi	13790 MPa
	G	1500 ksi	10343 MPa
	E	3600 ksi	24822 MPa
	$\nu$	0.2	0.2
Constants for Ultimate Yielding	$\alpha$	0.184	0.184
	$\gamma$	0.28 ksi	1.931 MPa
	$\delta = 3R$	1.070 ksi	7.378 MPa
Constants for Hardening	$\beta_a$	$4.961 \times 10^{-3}$	$4.961 \times 10^{-3}$
	$\eta_1$	$4.921 \times 10^{-1}$	$4.921 \times 10^{-1}$
	$\beta_b$	$6.2422 \times 10^{-1}$	$6.2422 \times 10^{-1}$
	$\eta_2$	$1.932 \times 10^{-1}$	$1.932 \times 10^{-1}$

1.0 psi = 6.89 kPa

TABLE 2 ULTIMATE MATERIAL CONSTANTS FOR STEEL-FIBER-REINFORCED CONCRETE FROM DIFFERENT STRESS PATH TESTS

		English Units	SI Units
Constants for Ultimate Yielding	$\alpha$	0.2215	0.2215
	$\gamma$	0.139 ksi	0.9577 MPa
	$\beta_{ult} = 3\alpha$	0.6645	0.6645
	$\delta = 3R$	1.743 ksi	12.01 MPa

1.0 psi = 6.89 kPa

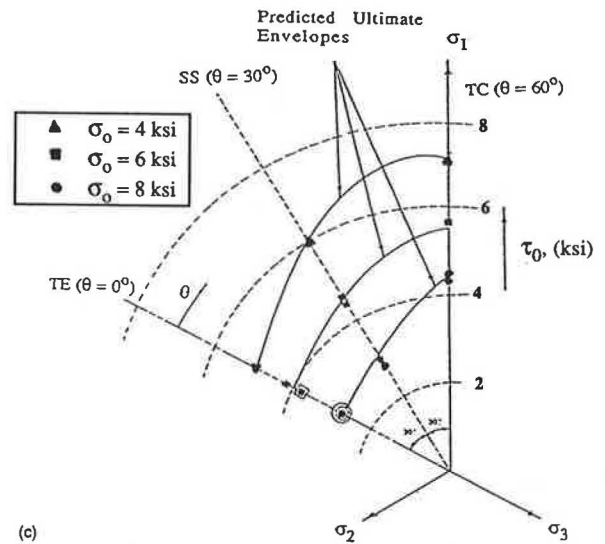
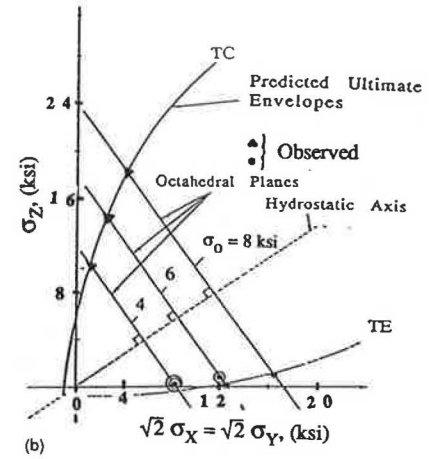
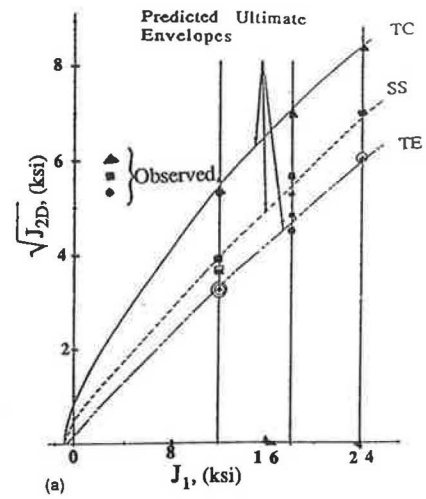


FIGURE 3 Ultimate and predicted ultimate envelopes (1.0 psi = 6.89 kPa): *a*, in  $(J_{2D})^{1/2} - J_1$  plane for steel-fiber-reinforced concrete; *b*, in triaxial plane for steel-fiber-reinforced concrete; *c*, in octahedral plane for steel-fiber-reinforced concrete.

pressed in terms of stress, stress increments, and the material constants (Tables 1 and 2).

The predicted responses for plain concrete and steel-fiber-reinforced concrete were compared with typical observed curves. Figures 1a and b show the ultimate envelopes in  $[J^I - (J_{2D})^{1/2}]$  and triaxial planes for plain concrete. Figure 1c shows comparisons between predictions and observations (plain concrete) for the triaxial extension ( $TE$ ,  $\sigma_o = 6$  ksi) test. Also, Figures 3a–c show comparisons between predictions and observations of steel-fiber-reinforced concrete for envelopes in the  $[J^I - (J_{2D})^{1/2}]$ , triaxial and octahedral planes, respectively.

These results indicate that the model can predict the stress-strain and the volumetric behavior satisfactorily. In this study, unloading and reloading were assumed to be elastic and linear as defined by the elastic constant ( $E$ ,  $\nu$ ).

## CONCLUSION

A general, yet simplified, model is proposed and used to model behavior of geological and engineering materials such as concrete, rocks, and soils as affected by complex factors such as state of stress, stress path, and volume change. It allows for continuously yielding and stress hardening, ultimate yield and cohesive and tensile strength components. A series of multiaxial laboratory tests conducted under various stress paths and initial multiaxial laboratory tests conducted under various stress paths and initial confinements was performed. The test results were used to derive material constants. The model was verified with respect to laboratory test data used for finding the constants and a complex circular stress path test not used for finding the constants. The model was found

to provide satisfactory predictions for the observed behavior of the plain concrete and steel-fiber-reinforced concrete.

## ACKNOWLEDGMENTS

Part of this investigation was supported by the Air Force Office of Scientific Research, Bolling Air Force Station, Washington, D.C., and the National Science Foundation.

## REFERENCES

1. Chen et al. Finite Element Analysis of Reinforced Concrete. In *Committee on Concrete and Masonry Structures*. Structural Division, ASCE, New York, N.Y., July 1982, pp. 34–137.
2. C. S. Desai and M. O. Faruque. A Constitutive Model for Geological Materials. *Journal of the Engineering Mechanics Division*, ASCE, Vol. 110, Sept. 1984, pp. 139–148.
3. M. R. Salami. Constitutive Modelling of Concrete and Rocks Under Multiaxial Compressive Loading. Ph.D. dissertation. Department of Civil Engineering and Engineering Mechanics, University of Arizona, Tucson, June 1986.
4. P. V. Lade. Three-Parameter Failure Criterion for Concrete. *Journal of the Engineering Mechanics Division*, ASCE, Vol. 108, No. EM5, Proc. Paper 17383, Oct. 1982.
5. R. Scavuzzo, H. V. Cornelius, K. H. Gerstle, H. Y. Ko, and T. Stankowski. *Stress-Strain Curves for Concrete Under Multiaxial Load Histories*. University of Colorado, Department of Civil, Environmental, and Architectural Engineering, Aug. 1983.
6. D. E. Egging. Constitutive Relations of Randomly Oriented Steel Fiber Reinforced Concrete Under Multiaxial Compression Loadings. M.S. thesis. University of Colorado, Department of Civil, Environmental, and Architectural Engineering, 1982.

---

*Publication of this paper sponsored by Committee on Mechanical Properties of Concrete.*